JACS
JOURNAL OF THE AMERICAN CHEMICAL SOCIETY

ARTICLE

pubs.acs.org/JACS

Peptoid Atropisomers

Bishwajit Paul,[†] Glenn L. Butterfoss,[‡,§] Mikki G. Boswell,[∥] P. Douglas Renfrew,[‡,§] Fanny G. Yeung,[∥] Neel H. Shah,[†] Christian Wolf,[∥] Richard Bonneau,[‡,§] and Kent Kirshenbaum*[,†]

[†]Department of Chemistry, [‡]Center for Genomics & Systems Biology, and Courant Institute of Mathematical Sciences, and [§]Department of Computer Science, New York University, New York, New York 10003, United States

[∥]Department of Chemistry, Georgetown University, Washington, D.C. 20057, United States

Supporting Information

ABSTRACT: We report the isolation of *N*-aryl peptoid oligomers that adopt chiral folds, despite the absence of chiral centers. Peptoid monomers incorporating ortho-substituted *N*-aryl side chains are identified that exhibit axial chirality. We observe significant energy barriers to rotation about the stereogenic carbon−nitrogen bond, allowing chromatographic purification of stable atropisomeric forms. We study the atropisomerism of *N*-aryl peptoid oligomers by computational modeling, NMR, X-ray crystallography, dynamic HPLC, and circular dichroism. The results demonstrate a new approach to promote the conformational ordering of this important class of foldamer compounds.

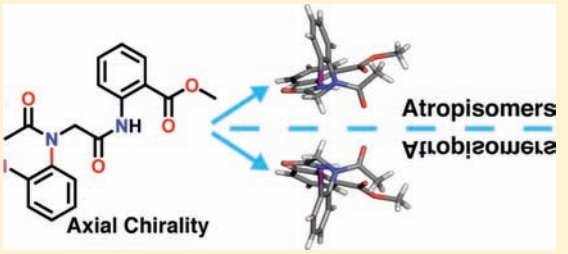

INTRODUCTION

Peptoids are a family of peptidomimetic oligomers composed of *N*-substituted glycine monomer units. An efficient solid-phase synthesis protocol enables the generation of peptoid oligomers bearing a specific sequence of highly diverse side chain groups.[1,2] Peptoids can exhibit a range of functions, such as self-assembly,[3−5] enantioselective catalysis,[6] intracellular transport,[7] molecular recognition,[8,9] antimicrobial activity,[10] and other biological activities.[11] The search for peptoids with new functions propels efforts to understand how particular peptoid sequences may encode for a specific conformation.[12−14] Until recently, the development of predictable sequence−structure−function relationships has been exclusively a characteristic of biological polymers.[15] This paradigm is now changing, as chemists are learning how to enforce the folding of peptoids, beta-peptides, aromatic oligoamides, and other "foldamer" compounds.[16]

Many of the critical attributes contributing to polypeptide folding are seemingly absent from the peptoid backbone. Peptoids feature tertiary amide linkages and therefore lack an intrinsic capacity for hydrogen bonding. In comparison with natural polypeptides, the absence of chiral centers may also increase peptoid conformational heterogeneity. Nevertheless, a judicious choice of peptoid side chains can promote the formation of stable secondary structures. For example, the incorporation of bulky *N*-alkyl side chains can enforce an energetic preference for *cis* (*Z*) amide bonds ($\omega = 0°$) [17] and also constrains the other two backbone dihedral angles φ and ψ (Scheme 1).[18] Previous studies have demonstrated that *N*-aryl side chains could similarly enforce a propensity for *trans* (*E*) omega bonds ($\omega = 180°$).[19,20] Through these complementary constraints, certain peptoid sequences can direct the formation of stable helical secondary structures: bulky *N*-alkyl side chains promote a polyproline I type helix,[12,21] and *N*-aryl side chains promote a polyproline II type (pp II) helix.[19] The peptoid backbone is generally flexible and lacks chiral centers. The achirality ineluctably leads to a racemic mixture of right- and left-handed helical structures. This shortcoming can be compensated by inclusion of chiral centers in the peptoid side chains. For example, the inclusion of *R* or *S* homochiral bulky *N*-alkyl side chains can determine a right- or left-handed peptoid helix.[12,22] Control of helical pitch in *N*-aryl peptoids, however, has not been demonstrated.

It is now possible to select peptoid side chains that reliably direct the backbone φ, ψ, and ω dihedral angles.[18] Side chain functional groups can engender peptoid conformational stability by means of hydrogen bonding,[14,20] stereoelectronic effects,[23,24] metal coordination,[4,8] or covalent bond formation via macrocyclization reactions.[25] Our attention is now focused on strategies to constrain the side chain (χ_1) dihedral angle, as these rotamers are an important source of conformational variability in polypeptide structures.[26] Following our initial studies of *N*-aryl peptoids, we were intrigued to evaluate whether the presence of bulky *ortho*-aryl substituents would provide a steric influence to constrain energetically accessible χ_1 angles in a predictable manner. The presence of congested anilide groups could give rise to atropisomerism,[27,28] leading to a novel structural influence for foldamer compounds.[29]

Atropisomerism is a stereochemical phenomenon in which hindered single-bond rotation leads to isolable stereoisomers.[30,31] For example, the restricted rotation about $C(sp^2)-C(sp^2)$ single bonds in *ortho*-substituted biphenyls can generate conformationally

Received: March 29, 2011
Published: June 02, 2011

Scheme 1. Peptoid Monomer and Oligomer[a]

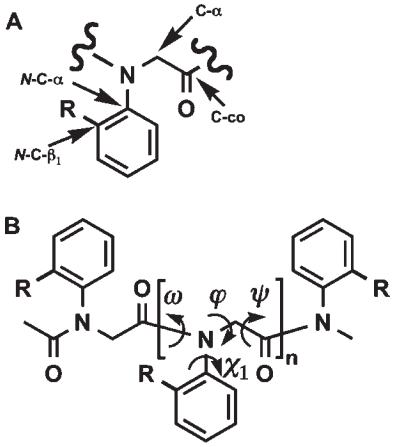

[a] (A) An *ortho*-substituted *N*-aryl glycine peptoid monomer showing atom labels. (B) Dihedral angles for a representative peptoid oligomer with an acetylated N-terminus.

Scheme 2. Atropisomerism in Biaryl and Nonbiaryl Systems[a]

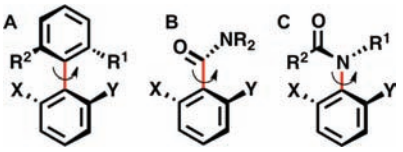

[a] (A) Classic biphenyl system. (B) Benzamide system. (C) Anilide system.

stable enantiomers that can be separated by chromatography or other means (Scheme 2A).[32] Ongoing studies of atropisomerism have led to fascinating examples of conformational control of organic compounds.[33−36] Atropisomers have also been evaluated as unusual enantioselective catalytic systems, establishing substantial practical significance.[37] Along with prototypical biaryl systems, nonbiaryl compounds can also exhibit atropisomerism, including nonplanar aromatic amides that are axially chiral due to restricted rotation about the aryl-carbon/nitrogen bond (Scheme 2B and C). This work seeks to extend the study of atropisomerism to control the conformation of biomimetic oligomeric molecules. Here, we report nuclear magnetic resonance (NMR), dynamic high-performance liquid chromatography (DHPLC), circular dichroism (CD), and X-ray crystallographic and computational studies of peptoid atropisomers.

RESULTS AND DISCUSSION

***N*-aryl Peptoid Synthesis.** We synthesized a series of simple monomeric peptoids (compound series **1**) incorporating various *N*-aryl side chains with methyl (Me), *tert*-butyl (*t*Bu), iodo (I), or carboxy methyl ester (ester) groups as *ortho*-substituents as well as the unsubstituted *N*-aryl peptoid monomer **1-H** (Scheme 3A). Compound series **1** was designed to feature *ortho*-substituents of varying steric bulk, particularly including the iodo and *tert*-butyl groups, as the corresponding anilides are known to form stable atropisomers.[27,36,38] To synthesize these peptoid monomers with good yields and purities, we employed slight modifications to previously reported protocols (see Supporting Information).[23,39] Briefly, synthesis began with nucleophilic displacement of

Scheme 3. Chemical Structures of *N*-aryl Peptoid Monomers and Dimeric and Trimeric *N*-aryl Peptoids[a]

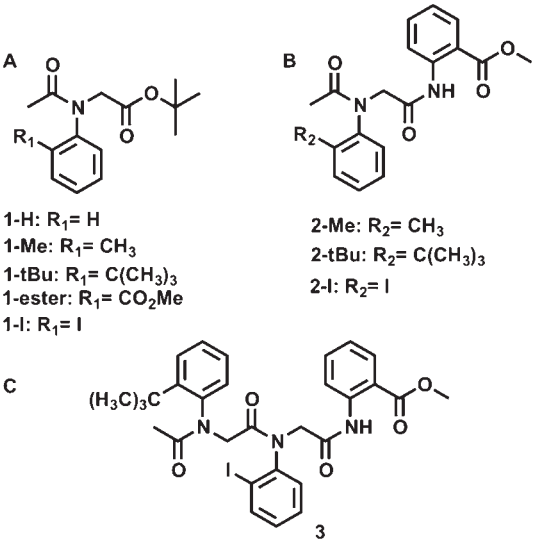

[a] (A) Chemical structure of *N*-aryl peptoid monomers. (B) Dimeric *N*-aryl peptoids. (C) Trimeric *N*-aryl peptoid. For the purpose of this study, the terms dimer and trimer are used to indicate the number of anilide side chain groups.

bromide from *tert*-butyl bromoacetate by various aromatic amines in refluxing conditions to obtain an *ortho*-substituted *N*-(*tert*-butylacetate)aniline. This was followed by acetylation of the N-terminus with acetyl chloride overnight at room temperature.

For the synthesis of peptoid oligomers, we adopted a solution-phase 'submonomer' synthesis cycle consisting of a modular and iterative two-step protocol (Scheme 4). Due to the poor nucleophilicity of *ortho*-subsituted aryl amines, the acylation step required modifications from standard submonomer synthetic procedures[1] as follows: For the first step, methyl anthranilate was coupled with activated bromoacetyl bromide at 0 °C, followed by gradual increase to room temperature (rt) to obtain *ortho*-substituted *N*-(2-phenyl)bromoacetamide derivatives. Next, the displacement of bromide by deactivated primary aromatic amines was conducted under refluxing conditions to obtain peptoid dimers. These two steps were repeated to obtain the sequence-specific *ortho*-substituted *N*-aryl peptoid trimer (see Supporting Information). The N-termini were acetylated using acetyl chloride to obtain peptoid dimers **2** and the trimer **3** (Scheme 3B and C). Crude peptoid compounds were purified by standard silica-gel column chromatography. The purity and identity of the products were confirmed by reversed-phase HPLC (RP-HPLC), NMR, and electrospray mass spectrometry (ESI-MS) (see Supporting Information).

Conformational Analysis of *N*-aryl Peptoid Monomers. *Ortho*-substituted *N*-aryl peptoids feature a flexible backbone and can potentially adopt a number of conformational states. Similar to the convention for polypeptides, the backbone dihedral angles are described as φ, ψ, and the amide bond ω (Scheme 1). Our previous report of *N*-aryl peptoids identified two low-energy backbone states, resembling either a left-handed polyproline II type (ppII) conformation with $(\omega, \varphi, \psi) \approx (180°, -75°, 160°)$ or its mirror image $(\omega, \varphi, \psi) \approx (180°, 75°, -160°)$.[19] The side chain can exhibit two predominating rotameric states ($\chi_1 \approx \pm 90°$), both placing the aryl ring orthogonal to the plane of

Scheme 4. Solution-Phase Synthesis of *N*-aryl Peptoid Oligomers

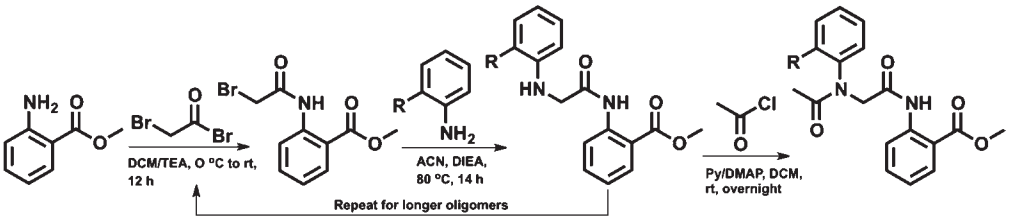

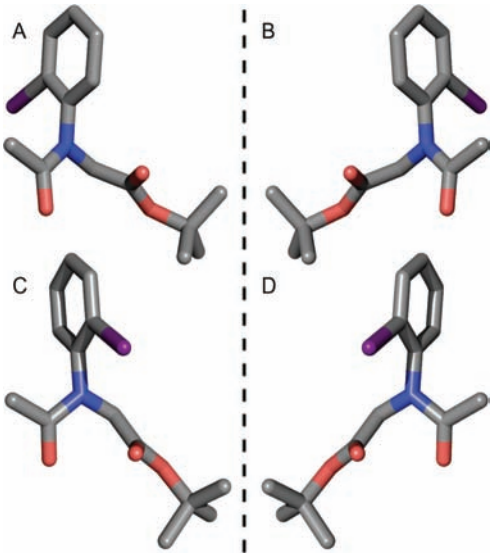

Figure 1. Low-energy conformational states of peptoid monomer **1-I**. Structure A is one atropisomer from the crystal unit cell, and B is its enantiomer. Structure C represents an alternative rotamer minimized at the HF/3-21G* level of theory, and D is its enantiomer.

Table 1. Dihedral Angles Observed by X-ray Crystallography of (*P*)-1-ester, (*P*)-1-I, and Their Enantiomers (*M*)-1-ester and (*M*)-1-I

peptoids	$\omega°$	$\varphi°$	$\psi°$	$\chi_1°$
(*P*)-**1-ester**	172.5	73.5	−167.2	118.1
(*M*)-**1-ester**	−172.5	−73.5	167.2	−118.1
(*P*)-**1-I**	175.8	76.9	−170.2	103.7
(*M*)-**1-I**	−175.8	−76.9	170.2	−103.7

the amide bond. For each peptoid monomer unit, four possible local energy conformations can therefore be expected (Figure 1A–D). Our initial characterization efforts were aimed at evaluating the relative energies and the dynamics of these conformers.

We obtained crystals of **1-ester** and **1-I** by slow evaporation from $CHCl_3$ at 4 °C. Both compounds were monoclinic and crystallized in the space group $P2_1/c$. Thus, the molecules were observed as enantiomeric pairs with *P* or *M* stereochemistry (see Supporting Information). The dihedral angles observed in the solid-state structure of **1-ester** and **1-I** are listed in Table 1. As expected, the *N*-aryl peptoid monomers **1-ester** and **1-I** include *trans*-amide bonds with ω = 172.5° and 175.8°, respectively. In each case, the other backbone dihedral angles (φ, ψ) fall within the range

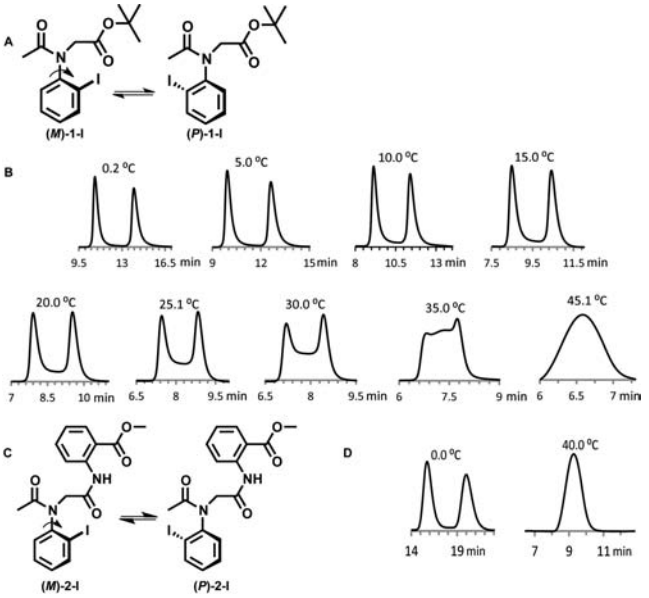

Figure 2. Restricted rotation about the anilide N–C bond allows separation of stable peptoid atropisomers. (A) Enantiomerization of peptoid monomer **1-I** between *M* and *P* stereochemical forms. (B) Chiral HPLC allows enantioseparation of **1-I** below 25 °C. Dynamic HPLC demonstrates enantioconversion at elevated temperatures. (C) Enantiomerization of peptoid dimer **2-I**. (D) Enantioseparation of **2-I**, along with enantioconversion at elevated temperature.

anticipated by our previous computational studies of *N*-aryl peptoids,[19] (73.5°, −167.2°) and (76.9°, −170.2°) for **1-ester** and **1-I**, respectively. These values are also in close agreement with previously reported *ortho*-hydroxyl and *ortho*-acetamide *N*-aryl peptoids.[20] In addition, the χ_1 dihedral angles for **1-ester** and **1-I** are 118.1° and 103.7°, respectively, within the range of previously predicted broad minima centered around ±90°.[19] These values place the aryl ring of the tertiary anilide perpendicular to the plane of the amide bond, with the side chain *ortho*-substituents of both **1-ester** and **1-I** pointing away from the following backbone carbonyl group, as depicted in Figure 1A and B.

Side Chain Rotational Barriers. For *ortho*-substituted *N*-aryl peptoids to exhibit atropisomerism, rotation around the *N*-aryl bond must be hindered (Scheme 2C). Restricted rotation around the χ_1 dihedral angle would render the backbone CH_2 groups to appear as magnetically nonequivalent CH_AH_B signals by NMR. One-dimensional (1D) NMR spectra were collected in $CDCl_3$ at rt for all peptoid monomers (**1-H**, **1-Me**, **1-*t*Bu**, **1-I**, and **1-ester**). For these compounds, the geminal methylene protons were observed to be magnetically nonequivalent at ambient temperature

dx.doi.org/10.1021/ja2028684 |*J. Am. Chem. Soc.* 2011, 133, 10910–10919

Table 2. Optimized Torsions and Energies of Peptoid Monomers 1-ester, 1-I, and 1-*t*Bu

					energy (kcal/mol)[a]			
peptoids	$\omega°$	$\varphi°$	$\psi°$	$\chi_1°$	B3LYP/LANL2DZ	B3LYP/6-31G* (3-21G*)[b]	M052X/6-31G* (3-21G*)[b]	MP2(full)/ 6-31G* (3-21G*)[b]
1-ester	179.9	76.7	−166.3	92.5	0.00	0.00	0.00	0.00
1-ester	170.2	94.4	−166.8	−83.2	1.66	1.81	1.32	0.52
1-I	176.4	−76.1	173.3	−97.6	0.00	0.00	0.00	0.00
1-I	178.9	−66.0	171.2	100.0	5.40	5.44	5.98	5.49
1-*t*Bu	173.1	−69.8	168.9	−99.6	0.00	0.00	0.00	0.00
1-*t*Bu	−171.4	−66.1	155.4	112.3	2.25	1.11	0.63	0.58

[a] Geometries were freely optimized in each minimum at the HF/6-31G* level of theory, except for **1-I** which was optimized at HF/3-21G*. [b] **1-ester** and **1-*t*Bu** energies are calculated with the 6-31G* basis set, and **1-I** energies are calculated with the 3-21G* basis set.

(with the exception of the unsubstituted compound **1-H** due to the symmetry around the χ_1 dihedral angle, see Supporting Information). These results are in accordance with studies of *ortho*-substituted anilides by Siddall and Mislow et al. conducted more than 40 years ago.[40] To further investigate the restricted rotational features around the *N*-aryl bond, we used variable temperature NMR (VT-NMR) in which an increase of temperature might allow sufficiently rapid interchange of side chain rotamers, resulting in coalescence of the NMR signals of the backbone methylene protons. However, no such coalescence was observed for **1-I** or **1-*t*Bu** up to 150 °C, indicating that the rotation around the χ_1 dihedral angle is slow on the NMR time scale (see Supporting Information). Similar significant rotational barriers have been previously observed in *ortho*-substituted anilides.[41]

Chromatographic and CD Studies of *N*-aryl Peptoid Monomers. If the energy barriers to interconversion of peptoid atropisomeric forms are significant, then it may be possible to separate the *M* and *P* stereoisomers at ambient conditions (Figure 2A).[35,42] We screened several chiral HPLC columns to separate the enantiomers of compounds **1-Me**, **1-*t*Bu**, **1-I**, and **1-ester**. We found that **1-*t*Bu** and **1-I** can be resolved by chiral HPLC. For example, **1-I** shows enantioseparation into (*M*)-**1-I** and (*P*)-**1-I**, during HPLC on a Whelk-O 1 chiral stationary phase (Figure 2B). Dynamic HPLC (DHPLC) can be performed at variable temperatures, providing a means to determine interconversion barriers of these compounds. Below 20 °C, baseline separation of **1-I** enantiomers was observed. At higher temperatures, however, more rapid interconversion between the enantiomers resulted in coalescence, and a single peak was observed at 45 °C. Computational fitting of the experimentally obtained DHPLC elution profiles gave an activation energy ($\Delta G^{\ddagger}$) of 21.5 kcal/mol at 25 °C. A van't Hoff plot of the DHPLC data obtained for **1-I** gave $\Delta H^{\ddagger}$ = 17.2 kcal/mol and $\Delta S^{\ddagger}$ = −14.4 cal/K mol, indicative of a highly organized transition state. In addition, the enantiomers of **1-*t*Bu** were isolated as (*M*)- and (*P*)-**1-*t*Bu** by semipreparative chiral HPLC on Chiralcel OD and showed mirror image CD spectra (see Supporting Information). These experimental results establish that *N*-aryl peptoids can form atropisomers that are stable and isolable.

Computational Analysis of *N*-aryl Peptoid Monomers. To elucidate the conformational preference of *ortho*-substituted *N*-aryl peptoids, we conducted ab initio quantum mechanics calculations. Table 2 shows the optimized torsions and the relative energies of the nonequivalent local minima of **1-ester**, **1-I**, and **1-*t*Bu**. The lowest energy conformations of **1-I** and **1-ester** agree with the geometries observed in the crystal structures (see Supporting Information). In both cases, the χ_1 preference is for the *ortho*-substituent to point away from the following carbonyl, as depicted in Figure 1A and B. Both **1-I** and **1-*t*Bu** contain bulky *ortho*-groups, but **1-I** is predicted to have a much larger energy difference between the χ_1 rotamers than **1-*t*Bu** (∼5 vs ∼1 kcal/mol, respectively) using various levels of theory. A possible origin for this difference may be repulsive interactions between the substantial electron density of the iodo group and the C-terminal carbonyl oxygen (alternatively, attractive interactions may also be manifested as "halogen bonds", vide infra). This notion is supported by similar strong rotamer preferences predicted for analogous electron-rich *ortho*-substituted *N*-aryl peptoids, i.e. *ortho*-halogens and *ortho*-carboxylate (see Supporting Information). This computational result suggests the physical origins for an energetic preference of the rotamer depicted in Figure 1A and B. Notably, the rotamer preference observed for the peptoids in this study is opposite to that previously observed for *ortho*-hydroxyl and *ortho*-acetamide *N*-aryl peptoids, which are capable of forming a hydrogen bond with the following carbonyl when they are in proximity.[20]

We further investigated the rotational barrier heights by computational studies. The complete conversion between *ortho*-substituted *N*-aryl peptoid atropisomeric states requires extensive rotation around both φ and χ_1. We estimated the energetic barriers to interconversion by calculating the individual barriers separately, assuming that coupled φ and χ_1 interconversion will have similar barriers. Using several model chemistries, we predicted the transition states (TS) for rotation about φ in **1-H** to be in the range of 7.3−8.5 kcal/mol for $\varphi \approx 0°$ and 7.4−9.0 kcal/mol for $\varphi \approx 180°$ (see Supporting Information). We also calculated the rotational barriers about χ_1 for minimal models of various *ortho*-substituted *N*-aryl peptoid side chains (Table 3). Notably, iodo and *tert*-butyl *ortho*-aryl susbtituents create very high χ_1 rotational barriers, in excess of 20 and 30 kcal/mol, respectively. These values are consistent with the large energy barriers required to isolate stable atropisomers and are comparable to the values determined by the DHPLC studies.[34,35,43]

Computational Studies of *N*-aryl Peptoid Dimers. We conducted further computational studies of *N*-aryl peptoid dimers. For the compound family **2**, the C-terminal backbone nitrogen is a secondary anilide, allowing the adjoining phenyl ring to be coplanar with the amide bond. There are two low-energy conformations of ψ in vicinity of 15° and 180°. This feature, along with the two local minima for each φ and χ_1 angle, leads to at least eight local energy minimum conformations (Figure 3). Ab initio models predict the lowest energy geometries to be a compact form (Figure 3D) and a more extended form (Figure 3A), in which ψ is rotated (see Supporting Information). In both geometries, the *ortho* group is disposed away from the following backbone

carbonyl, which is also the low-energy conformation predicted and observed for the monomer compounds. The compact conformation is favored by over 1 kcal/mol relative to other low-energy structures at both the M052X/6-31G* (**2-Me**) and M052X/3-21G* (**2-Me**, **2-I**) levels of theory (see Supporting Information).

Crystallographic Analysis of *N*-aryl Peptoid Dimers. We prepared peptoid dimers **2-Me**, **2-*t*Bu**, and **2-I** to evaluate the potential for atropisomeric behavior in *N*-aryl peptoid oligomer systems. Crystals of peptoid dimers **2-Me** and **2-I** were obtained by slow evaporation from $CHCl_3$ overnight at rt. X-ray diffraction studies showed that the dimer **2-I** and **2-Me** each form an enantiomeric pair within the crystal unit cell. These structures correspond to the lowest energy conformation predicted by the ab initio modeling ((*M*)-**2-I** and the enantiomer (*P*)-**2-I**, see Figure 3D). The *N*-aryl peptoid dimers **2-Me** and **2-I** form *trans* amide bonds with $\omega = 179.2°$ and 178.6°, respectively. The other backbone dihedral angles (φ, ψ) of **2-Me** and **2-I** are (−85.0°, 6.43°) and (−102.3°, 47.1°), respectively (Table 4). Additionally, the χ_1 dihedral angles at the tertiary anilide positions of **2-Me** and **2-I** are −80.4° and −101.8°, respectively. For both dimers, intramolecular hydrogen bonding is evident between the amide NH group and the carbonyl oxygen of the side chain ester at the C-terminus. The side chains exhibit distinct rotamer preferences. For the C-terminal secondary anilide, the aryl ring is coplanar with the amide bond ($\chi_1 \approx \pm 180°$), allowing hydrogen-bond formation. As expected, for the N-terminal tertiary anilide, the aryl ring is perpendicular to the amide plane ($\chi_1 \approx \pm 90°$).

Further analysis of the crystal structure of **2-I** reveals that the iodine is in close proximity (3.0 Å) to the carbonyl oxygen of an adjacent molecule in the crystal lattice. The angle formed between the C−I bond and the carbonyl oxygen is 171.3° (see Supporting Information). This constitutes a Lewis acid/base pair interaction for compound **2-I** and indicates the capability for peptoids to form 'halogen bonds'.[44]

Unexpectedly, we were also able to observe in the solid state the presence of a side chain rotameric conformation of **2-I** with low occupancies (~2%). This minor form could be detected due to the anomalous scattering of the heavy iodine atom. The χ_1 dihedral angle for this minor conformer was 107.9° and is modeled in Figure 3B. Thus, the peptoid dimers may exhibit some conformational heterogeneity of the side chain rotamers.

NMR Analysis of *N*-aryl Peptoid Dimers. NMR spectroscopy was used to analyze the solution structures of all dimers (**2-Me**, **2-*t*Bu**, and **2-I**) in $CDCl_3$ at rt. The 1-D ^1H and ^{13}C spectra show well-resolved peaks along with a one-to-one correspondence between the observed NMR peaks and the expected chemical shifts

Table 3. Calculated Transition State Energies for χ_1 Rotation in a Series of Peptoid Analogues[b]

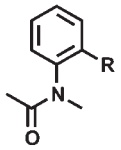

B3LYP/3-21G*(B3LYP/6-311+G(2d,p)) Energy (kcal/mol)

R=	$\chi_1 = \sim 0°$	$\chi_1 = \sim 180°$
H	17.7 (15.5)	17.7 (15.5)
Me	*N.A.*[a]	19.7 (19.3)
I	23.0	21.1
tBu	*N.A.*[a]	32.2 (30.7)

[a] Calculations did not converge on a saddle point in these regions. [b] TS energies are shown relative to the energy of the freely optimized structure. Geometries are optimized at the HF/6-31G* level (except for the iodo compound which is optimized at B3LYP/3-21G*).

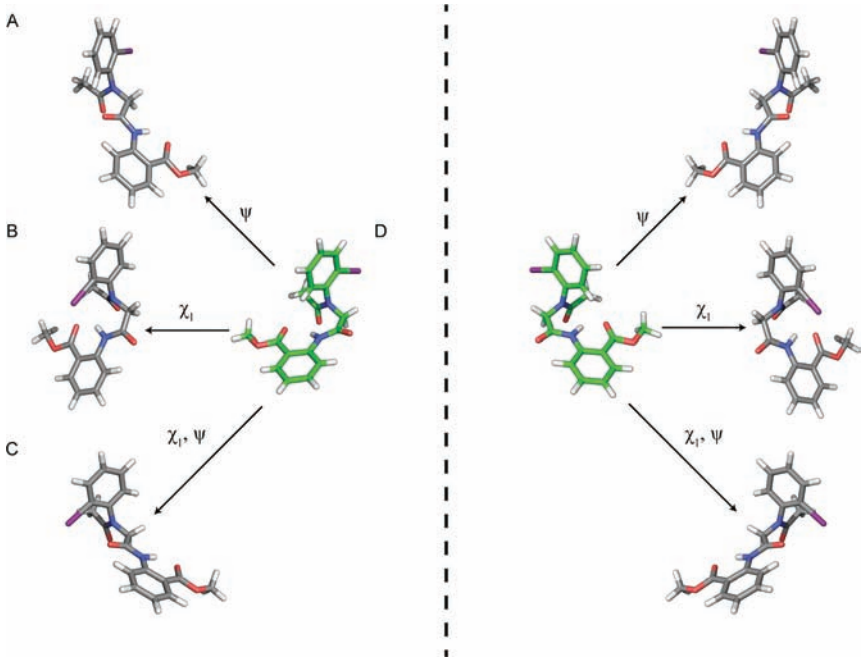

Figure 3. Low-energy conformational states of peptoid dimer **2-I**. The major conformational state observed in the crystal structure is depicted in D. An additional three low-energy conformational states of **2-I** can be obtained upon rotations about ψ (A), χ_1 (B), or both ψ and χ_1 (C). For each conformation, an enantiomeric structure can be observed or predicted (right panel). Green structures are experimental, and gray structures are optimized at the HF/3-21G* level of theory.

Table 4. Dihedral Angles Observed from the X-ray Crystallography for Peptoid Dimers (*M*)-2-Me, (*M*)-2-I, and the Enantiomers (*P*)-2-Me and (*P*)-2-I

peptoids	$\omega°$	$\varphi°$	$\psi°$	$\chi_1°$
(*M*)-**2-Me**	179.2	−85.0	6.43	−80.4
(*P*)-**2-Me**	−179.2	85.0	−6.43	80.4
(*M*)-**2-I**	178.6	−102.3	47.1	−101.8
(*P*)-**2-I**	−178.6	102.3	−47.1	101.8

(see Supporting Information). We also observed a distinct peak for the amide hydrogen, which was significantly downfield shifted (δ = 11.5 ppm). This result is consistent with the crystallographic data (vide supra), suggesting that the amide proton is engaged in intramolecular hydrogen bonding with the side chain carbonyl of the ester group at the C-terminus. To gain further insight into the conformational preference of the peptoid dimers in the solution state, we evaluated compound **2-I** by $^1H-^1H$ correlation spectroscopy (COSY) and nuclear Overhauser effect spectroscopy (NOESY). The $^1H-^1H$ COSY was carried out on **2-I** to unambiguously assign aromatic proton chemical shifts, as they show readily distinguishable through-bond cross-peaks (see Supporting Information). 2D-NOESY was used to gauge interproton distances and to assess the solution-phase behavior of **2-I**. Figure 4 highlights the key cross-peaks observed in **2-I**. The presence of a strong NOE between the acetyl-methyl group and the *ortho*-hydrogen of the N-terminal anilide, along with the absence of an NOE between the acetyl-methyl and backbone methylene protons, strongly indicates the presence of a *trans* amide bond at the N-terminal anilide.[19,20] Notably, a strong cross-peak was observed between the C-terminal amide hydrogen and one of the magnetically nonequivalent protons (H_a/H_b), while a slightly weaker NOE was observed with the other one (H_b/H_a), further substantiating the diastereotopic behavior of the methylene hydrogens in the *N*-aryl peptoid dimer (see Supporting Information). An NOE cross-peak was also observed between the *ortho*-hydrogen of the N-terminal anilide with the amide proton of the C-terminal anilide. This cross-peak strongly supports the notion that **2-I** has a compact solution structure similar to the solid state (Figure 3D) and does not adopt an extended backbone structure (as depicted in Figure 3A) or the alternate χ_1 rotamers (as depicted in Figure 3B and C), as these would most likely preclude observation of a strong NOE cross-peak (see Supporting Information).

DHPLC and CD Studies of *N*-aryl Peptoid Dimers. Chiral HPLC studies of peptoid dimers showed that **2-*t*Bu** and **2-I** could be separated into enantiomers at low temperatures. The enantiomers (*M*)-**2-I** and (*P*)-**2-I** were separated on Chiralcel OD at 0 °C. Peak coalescence was observed at 40 °C, however, due to rapid enantiomerization at elevated temperatures (Figure 2C, D). Computational analysis of the DHPLC elution profiles yielded an enantiomerization barrier, $\Delta G^{\ddagger}$, of 21.5 kcal/mol at 25 °C . The corresponding enthalpy of activation ($\Delta H^{\ddagger}$ = 17.8 kcal/mol) and entropy of activation ($\Delta S^{\ddagger}$ = −12.2 cal/K mol) were obtained by van't Hoff plot analysis. As expected, the enantiomerization barrier of the *N*-aryl peptoid dimer **2-I** is equivalent to the monomer **1-I**, suggesting that conformational stability is an intrinsic property of the congested tertiary anilide groups and is determined primarily by local interactions. As observed for **1-*t*Bu**, the dimer **2-*t*Bu** could be separated and isolated by semipreparative HPLC on Chiralpak AD. The enantioseparation was verified by the mirror image CD spectra obtained for the two enantiomeric forms of (*M*)-**2-*t*Bu** and (*P*)-**2-*t*Bu** (Figure 5).

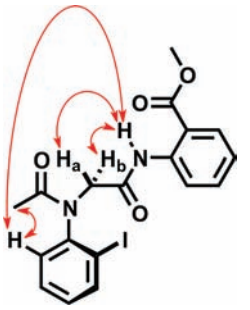

Figure 4. Key cross-peaks observed in NOESY spectra for **2-I** (shown as double-headed arrows).

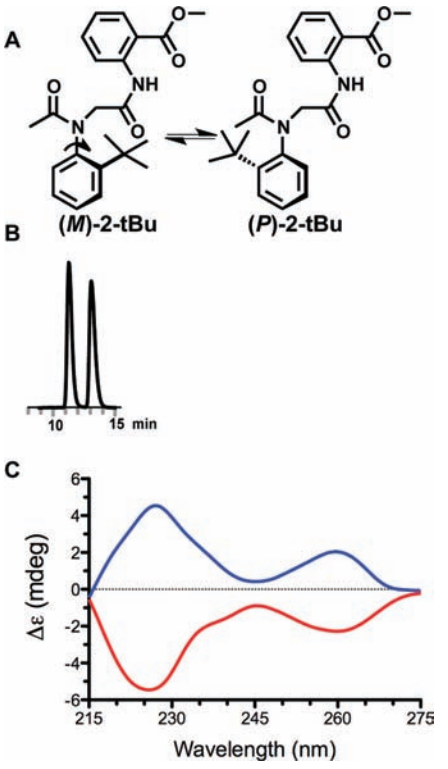

Figure 5. Chiral HPLC enantioseparation of **2-*t*Bu**. (A) Enantiomerization of **2-*t*Bu**. (B) Enantioseparation of **2-*t*Bu** at rt. (C) CD spectra of the first eluted enantiomer (red) and the second eluted enantiomer (blue).

Structural Analysis of an *N*-aryl Peptoid Trimer. The *N*-aryl peptoid trimer **3** includes two side chains capable of exhibiting atropisomerism at the tertiary anilide positions. In particular, compound **3** includes axial chirality at the *N*-aryl side chains incorporating an *ortho*-iodo and an *ortho-tert*-butyl substituent. The possibility for rotational isomers at both anilide positions can give rise to two pairs of enantiomers (Figure 6A). We evaluated the solution-state structure of peptoid trimer **3** in $CDCl_3$ at rt using NMR spectroscopy. The 1D NMR spectra of **3** show at least two major conformations with a ratio of 2:1 along with several minor conformers producing significant numbers of overlapping NMR peaks (see Supporting Information). Moreover, the RP-HPLC profile of recrystallized **3** shows two peaks in the chromatogram, also supporting the presence of diastereomeric forms of the peptoid trimer **3** (see Supporting Information).

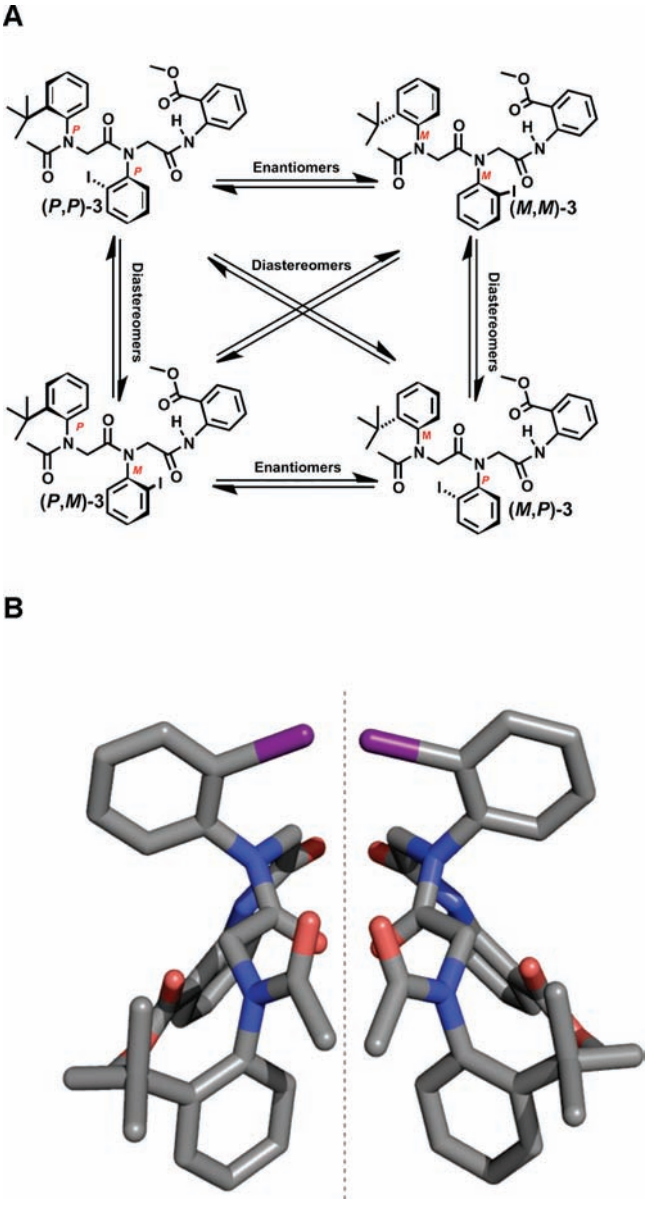

Figure 6. Conformations of *N*-aryl peptoid trimer **3**. (A) The possible stereoisomers and their relationships. (B) The predominant structure in the solid state shows the enantiomeric pair (*P*,*P*)-**3** and (*M*,*M*)-**3** (hydrogen atoms have been removed for clarity).

Further structural characterization of **3** was conducted by X-ray crystallography. A solution of trimer **3** in $CHCl_3$ was allowed to evaporate at rt overnight, forming block-shaped crystals in the $P2_1/c$ space group. Hence, the peptoid trimer **3** exists as enantiomeric pairs (*M*,*M*)-**3** and (*P*,*P*)-**3** within the unit cell (Figure 6B). The dihedral angles observed in the solid-state structure are listed in Table 5. We observed that the dihedral angles (ω, φ, ψ) were (178.9°, 80.4°, −169.0°) for the *tert*-butyl-anilide and (−179.0°, 79.2°, 4.70°) for the iodo-anilide position. In addition, the χ_1 dihedral angles are 98.6° and 101.3° at the *tert*-butyl- and iodo-anilide positions, respectively. Notably, the iodo-anilide position includes a significant deviation of the ψ dihedral angle from a ppII type conformation. This deviation from canonical pp II dihedral values is presumably due to the presence of the C-terminal secondary anilide group that similarly alters the

Table 5. Dihedral angles observed for *N*-aryl peptoid trimer (*P*,*P*)-3

peptoid residues	ω°	φ°	ψ°	χ_1°
(*P*-*t*Bu)-**3**	178.9	80.4	−169.0	98.6
(*P*-I)-**3**	−179.0	79.2	4.70	101.3

conformational preferences of the terminal ψ angle for the peptoid dimers (**2-I** and **2-Me**, Table 4). We also found that the C-terminal secondary anilide forms an intramolecular hydrogen bond with the carbonyl of the side chain ester group, and the corresponding aromatic ring is coplanar with the amide bond.

Like the peptoid dimer **2-I**, the rotamer of peptoid trimer **3** also shows an intermolecular Lewis acid/base interaction (see Supporting Information). The distance between the Lewis acid (iodine group) and the Lewis base (carbonyl oxygen) is 2.96 Å. The observed angle of 176.8° is also within halogen bonding parameters. The presence of this interaction in both dimeric and trimeric peptoids suggests that halogen bonding may be useful for the design of higher order structure in peptoids.[3]

As observed for the peptoid dimer **2-I**, we were also able to detect the presence of additional side chain rotamers of peptoid trimer **3** with low population density (∼2%). The χ_1 dihedral angles at the *tert*-butyl- and iodo-anilide positions are 98.6° and −100.4°, respectively. Peptoid trimer **3** features axial chirality at both the *tert*-butyl- and iodo-aryl side chains. For such oligomers with multiple stereogenic sites, the presence of a particular stereoisomer at one monomer position may influence the relative energy of stereoisomers at neighboring positions.[45] A peptoid oligomer incorporating a discrete stable stereogenic center could bias the preferential formation of a desired backbone conformation within a population of otherwise dynamic atropisomeric forms.[46] Future studies will evaluate the induction of chiral information in hybrid oligomers comprising both *N*-alkyl and *N*-aryl peptoid units.

Conclusions. We demonstrate that a chiral folded oligomer can be obtained by assembly of monomers lacking chiral centers. Peptoids bearing bulky *ortho*-substituted *N*-aryl side chains exhibit axial chirality, due to restricted rotation about the congested tertiary anilide positions. For peptoids including *ortho*-iodo or *ortho*-*tert*-butyl anilide groups, the energy barrier for rotation is sufficiently high to permit the chromatographic isolation of stable atropisomeric forms exhibiting mirror-image CD spectra. At elevated temperatures, *N*-aryl peptoid atropisomers undergo enantioconversion. X-ray crystal structures reveal details of the atropisomeric forms of *ortho*-substituted *N*-aryl peptoid monomers, dimers, and a trimer. Atropisomeric conformers of the peptoids are observed as enantiomeric pairs in the solid state. The peptoid conformations feature *trans* amide bonds and side chain rotamers in which the aryl groups are orthogonal to the plane of the amide bonds. Both intramolecular hydrogen and halogen bonding are observed in the crystal structure. The presence of two sites of axial chirality in the peptoid trimer yields diastereomeric conformers.

Our results show that the stereochemical features of folded *N*-aryl peptoid oligomers can be dynamic, as opposed to the stereochemistry of peptides and proteins, which is essentially static. We have previously shown the ability for peptoids to undergo backbone or side chain conformational rearrangements triggered by changes in pH[47] or by photoisomerization.[48] Future studies may yield functional peptoid structures that interconvert between stereochemical forms in response to external stimuli.[49]

EXPERIMENTAL SECTION

General Methods. All reagents and solvents were purchased from commercial sources and used without further purification. Thin-layer chromatography (TLC) was performed on precoated UV active silica gel. Silica gel (40−63 μm, Sorbent Technologies) was used for column chromatography.

Materials. Bromoacetyl bromide, aniline, 2-methylaniline, 2-*tert*-butylaniline, 2-iodoaniline, methylanthranilate, dimethylaminopyridine (DMAP), and triethylamine (TEA) were purchased from Sigma-Aldrich (St. Louis, MO). *N*,*N*-diisopropylethylamine (DIEA) and pyridine (Py) were purchased from Alfa-Aesar. Trifluoroacetic acid was purchased from Acros Organics. Anhydrous solvents, such as chloroform, acetonitrile (ACN), ethyl acetate (EtoAc), and dichloromethane (DCM) were purchased from commercial sources and used without further distillation.

Synthesis of Peptoid Monomers (1-H, 1-Me, 1-*t*Bu, 1-I, 1-ester). *Displacement Step.* To a solution of *tert*-butyl bromoacetate (550 μL, 3.72 mmol) and diethyl isopropyl amine (DIEA, 6 mL, 33.84 mmol) was added the aniline or aniline derivative (900 mg, 10.7 mmol) in acetonitrile. The reaction was then subjected to reflux for 14 h. Subsequently, the solution was cooled to rt followed by removal of solvent under reduced pressure in rotatory evaporator. The crude mixture was then subjected to silica gel column chromatography in a *n*-hexane/EtoAc to obtain the *N*-(*tert*-butyl acetate) aniline or aniline derivative.

Acetylation Step. The typical scale for this step was between 1 and 2 mmol. *N*-(*tert*-butyl acetate) aniline or its derivative was treated with pyridine (1.2 mmol) along with the addition of catalytic amounts of DMAP (∼0.5 mg) in dichloromethane (DCM) as solvent. The acetyl chloride (2−2.5 mmol) was then added in dropwise manner at rt with continued stirring and left to react overnight. Solvent was removed under reduced pressure and then subjected to silica gel column chromatography in a *n*-hexane/EtoAc mixture to obtain the pure compounds. Products were analyzed and confirmed by NMR and mass spectrometry (see Supporting Information). The desired compounds were isolated in the following yields over two steps: **1-H** (50%); **1-Me** (52%); **1-*t*Bu** (55%); **1-ester** (54%); and **1-I** (50%).

Synthesis of *N*-aryl Peptoid Dimers (2-I, 2-*t*Bu, 2-Me). *Bromoacetylation Step.* Methyl anthranilate (1.5 g, 10 mmol) was dissolved in DCM followed by addition of triethyl amine (1.4 mL, 10 mmol) under nitrogen at 0 °C. The reaction was stirred for 15 min at 0 °C before the addition of bromoacetyl bromide. Bromoacetyl bromide (1.4 mL, 15.9 mmol) was added dropwise for 10 min. An immediate change was observed from colorless to yellow solution, and the reaction mixture was allowed to stir overnight at rt. The solvent was removed under reduced pressure to afford a crude oil, which was purified by column chromatography in a *n*-hexane/EtoAc mixture.

Displacement Step. In a round-bottom flask, 1 mmol of *N*-(2-phenyl) bromoacetamide derivatives was taken in acetonitrile followed by addition of *ortho*-substituted amine (1.1 mmol) in the presence of DIEA (5 mmol) as base. The mixture was then subjected to reflux condition for 12 h. After the removal of solvent under reduced pressure, the compound was then subjected to silica gel column chromatography in a *n*-hexane/EtoAc mixture.

Acetylation Step. The typical scale for the next step was ∼1 mmol. In this step the compound was treated with pyridine (1.2 mmol) along with a catalytic amount of DMAP (∼0.5 mg) followed by addition of the DCM solvent at room temperature. The acetyl chloride (2.5 mmol) was then added in a dropwise manner at rt, and the reaction was stirred overnight. Upon removal of the solvent under reduced pressure, the product was then subjected to silica gel column chromatography in a *n*-hexane/EtoAc mixture to obtain the pure compound. The final compounds were analyzed and characterized by NMR and mass spectrometry. The desired compounds were isolated in the following yields over three steps: **2-Me** (24%); **2-*t*Bu** (20%); and **2-I** (15%).

Synthesis of *N*-aryl Peptoid Trimer 3. The synthesis of the trimer was performed following the same protocol as for the dimers, in which iterative bromoacetylation and displacement steps were conducted prior to final acetylation. The overall isolated yield of the trimer **3** was ∼10%.

Peptoid Characterization and Purification. Peptoid oligomers were characterized by analytical RP-HPLC using an analytical C_{18} column (Peeke Scientific, 5 μm, 120 Å, 2.0 × 50 mm) on a Beckman Coulter Gold HPLC system. Products were detected by UV absorbance at 214 nm during a linear gradient from 5 to 95% solvent B (0.1% of trifluoroacetic acid in HPLC-grade acetonitrile) in solvent A (0.1% of trifluoroacetic acid in HPLC-grade water) in 10 min with a flow rate of 0.7 mL.min^{-1}. The expected molecular mass of each product was confirmed using liquid chromatography-mass spectrometry (LC-MS) on an Agilent 1100 series LC/MSD trap XCT with an electrospray ion source in positive ion mode.

Peptoid products were purified to >95% purity, as assessed by NMR after silica gel column purification, and the peptoid **1-*t*Bu** was purified by using the same RP-HPLC apparatus described above with a preparatory C_{18} column. Products were detected by UV absorbance at 230 nm during linear gradient from 5 to 95% solvent B in solvent A in 50 min with a flow rate of 2.5 mL.min^{-1}. Compounds were then lyophilized before further characterization.

NMR Spectroscopy. Using either a Bruker 400 MHz NMR or a Bruker 500 MHz NMR spectrometer, 1D proton spectra were obtained. All ^{13}C NMR were recorded at 100 MHz. Chemical shifts are reported in parts per million (ppm, δ). Couplings are reported in Hertz. NOESY and H−^{1}H COSY experiments were performed using a 500 MHz instrument and were referenced to solvent. Except for the temperature-dependent ^{1}H NMR experiment, all NMR experiments were carried out at 25 °C.

NMR Analyses for Peptoids 2-I, 3. NOESY experiments on **2-I** in $CDCl_3$ were performed at 25 °C using the following parameter values: size of fid (TD) = 2048, 128; number of scans (NS) = 32; number of dummy scans (DS) = 4; mixing time (D8) = 800 ms; acquisition time (AQ) = 0.17 s; and relaxation delay = 1.5 s. ^{1}H−^{1}H COSY experiments on **2-I** in $CDCl_3$ were performed at 25 °C using the following parameters: TD = 2048, 192; NS = 40; DS = 4; AQ = 150 ms; and relaxation delay (D1) = 1.5 s. The concentration of the solution was 30 mM.

X-ray Crystallography. All software and sources of the scattering factors are contained in the program suite SHELXL. The intensity data collections were conducted with a Bruker SMART APEXII CCD area detector on a D8 goniometer at 100 K. The temperature during the data collection was controlled with an Oxford Cryosystems Series 700 plus instrument. Preliminary lattice parameters and orientation matrices were obtained from three sets of frames. Data were collected using graphite-monochromated and 0.5 mm MonoCap-collimated Mo−K_α radiation (λ = 0.71073 Å) with the ω scan method. Data were processed with the INTEGRATE program of the APEX2 software for reduction and cell refinement. Multiscan absorption corrections were applied by using the SCALE program for area detector. The structure was solved by the direct method and refined on F^2 (SHELXTL). Nonhydrogen atoms were refined with anisotropic displacement parameters, and hydrogen atoms on carbons were placed in idealized positions (C−H = 0.93 or 0.96 Å) and included as riding with U_{iso}(H) = 1.2 or 1.5 U_{eq}(non-H).

Crystallization of 1-ester. Roughly 10 mg of purified **1-ester** was dissolved in 1 mL of $CHCl_3$. The peptoid solution was filtered with a 0.5 μm stainless steel fritted syringe tip filter (Upchurch Scientific). The resulting solution was then allowed to evaporate slowly at 4 °C to form a block-shaped colorless crystal.

Crystallographic Data. $C_{16}H_{21}NO_5$, colorless block crystal, monoclinic, $P2_1/c$, a = 8.6027(7) Å, b = 10.4781(8) Å, c = 17.9484(14) Å, β = 96.0170(10)°, V = 1609.0(2) Å^3, Z = 4, T = 100(2) K, and ρ_{calc} = 1.269 g/cm^3.

Crystallization of 1-I. Roughly 10 mg of purified **1-I** was dissolved in 1 mL of $CHCl_3$. The peptoid solution was filtered with a 0.5 μm stainless steel fritted syringe tip filter. The resulting solution was then allowed to evaporate slowly at 4 °C to form a plate-shaped colorless crystal.

Crystallographic Data. $C_{14}H_{18}INO_3$, plate-shaped colorless crystal, monoclinic, $P2_1/c$, a = 9.0692(8) Å, b = 10.1549(9) Å, c = 17.5809(16) Å, β = 101.0230(10)°, V = 1589.3(2) Å^3, Z = 4, T = 100(2) K, and ρ_{calc}= 1.568 g/cm^3.

Crystallization of 2-Me. Roughly 10 mg purified of **2-Me** was dissolved in $CHCl_3$. The peptoid solution was filtered with a 0.5 μm stainless steel fritted syringe tip filter. The solution was then allowed to evaporate slowly at rt to obtain plate-shaped colorless crystals.

Crystallographic Data. $C_{19}H_{20}N_2O_4$, plate-shaped colorless crystal, orthorhombic, *Pbca*, a = 10.5493(15) Å, b = 16.050(2) Å, c = 20.088(3) Å, $\alpha = \beta = \gamma$ = 90°, V = 3401.4(8) Å^3, Z = 8, T = 100(2) K, and ρ_{calc} = 1.329 g/cm^3.

Crystallization of 2-I. The purified compound **2-I** was dissolved in chloroform to a concentration of 10 mM. The peptoid solution was filtered with a 0.5 μm stainless steel fritted syringe tip filter. The solution was then allowed to evaporate slowly at rt to obtain plated-shaped colorless crystals.

Crystallographic Data. $C_{18}H_{17}IN_2O_4$, plate-shaped colorless crystal, triclinic, $P\bar{1}$, a = 7.9952(2) Å, b = 16.050(2) Å, c = 20.088(3) Å, α = 93.2104(10)°, β = 94.7131(10)°, γ = 97.9838(5)°, V = 873.65(8) Å^3, Z = 2, T = 100(2) K, and ρ_{calc}= 1.719 g/cm^3.

Crystallization of 3. The purified compound **3** was dissolved in chloroform to a concentration of roughly 10 mM. The peptoid solution was filtered with a 0.5 μm stainless steel fritted syringe tip filter. The solution was then allowed to evaporate slowly at rt to obtain block-shaped colorless crystals.

Crystallization Data. $C_{30}H_{32}IN_3O_5$, block, colorless crystal, monoclinic, $P2_1/c$, a = 8.1287(3) Å, b = 20.4002(8) Å, c = 17.2759(7) Å, β = 92.1300(10)°, V = 2862.83(19) Å^3, Z = 4, T = 100(2) K, and ρ_{calc}= 1.488 g/cm^3.

Computational Studies. All ab initio quantum mechanics calculations used Gaussian 03 (Supporting Information for full references list). The levels of theory and basis sets are indicated in the main text. The TS optimizations began with starting structures thought to be in the conformational vicinity of the TS and used the "TS Opt=(TS,NoEigenTest, CalcFC) nosym" options. The SCF = tight option was specified in all calculations.

Chiral HPLC and CD analysis of *N*-aryl Peptoids: 1-I. The analytical enantioseparation was conducted on a (*S*,*S*)-Whelk-O 1 CSP using hexanes/IPA (90/10 v/v) as the mobile phase at a flow rate of 1 mL/min. The enantiomers were detected by UV absorbance at 230 nm.

1-*t*Bu. The analytical separation was performed on a Chiralcel OD CSP using hexanes/IPA (95/5 v/v) as the mobile phase at a flow rate of 1 mL/min. The enantiomers were detected by UV absorbance at 254 nm. The semipreparative enantioseparation was conducted at rt using a sample concentration of 0.96 mg/mL and an injection volume of 100 μL. After the isolation of the two enantiomers, CD spectroscopy was conducted with sample concentrations of 4.8 mM.

Enantioseparation of 2-I. The analytical separation was performed on a Chiralcel OD CSP using hexanes/EtOH (85/15 v/v) as the mobile phase at a flow rate of 1 mL/min. The enantiomers were detected by UV absorbance at 230 nm.

Semipreparative Chromatography of 2-*t*Bu. The analytical separation was performed on Chiralpak AD using hexanes/IPA (90/10 v/v) as the mobile phase at a flow rate of 1 mL/min. The enantiomers were detected by UV absorbance at 254 nm. The semipreparative enantioseparation was conducted at rt using a sample concentration of 1.59 mg/mL and an injection volume of 50 μL. After the isolation of the two enantiomers, CD spectroscopy was conducted with sample concentrations of 4.0 mM.

■ ASSOCIATED CONTENT

Supporting Information. Complete reference of Gaussian 03; NMR and mass spectrometry characterization of synthesized peptoid monomers (**1-H**, **1-Me**, **1-*t*Bu**, **1-I** and **1-ester**), dimers (**2-Me**, **2-I** and **2-*t*Bu**), and trimer **3**; mass spectrometry and RP-HPLC characterization data for all peptoids; additional representations of the crystal structures of **1-ester**, **1-I**, **2-Me**, **2-I**, and trimer **3**; halogen bonding features (distance and angle) of **2-I** and **3**; 1D and 2D NMR spectra of compounds all peptoid monomers, dimers, and trimer; crystal and computationally evaluated conformers of **2-I**; additional computational data; rotational barrier across ψ and χ, respectively; dynamic HPLC, enantioconversion, and computational fitting of elution profiles to obtain van't Hoff plots of **1-I** and **2-I**; enantioseparation and CD analysis of **1-*t*Bu**. This material is available free of charge via the Internet at http://pubs.acs.org.

■ AUTHOR INFORMATION

Corresponding Author
kent@nyu.edu

■ ACKNOWLEDGMENT

This work was supported by a National Science Foundation CAREER Award (CHE-0645361). Funding from the NSF under CHE-0910604 is also gratefully acknowledged. NYU is the recipient of an NCRR/NIH research facilities improvement grant (C06RR-165720). We thank the NYU Molecular Design Institute for access to the Bruker SMART APEXII X-ray diffractometer and Dr. Chunhua (Tony) Hu for his help with data collection and structure determination. We thank Arjel Bautista, Chin Lin, Barney Yoo, and James Canary for their helpful discussions and suggestions.

■ REFERENCES

(1) Zuckermann, R. N.; Kerr, J. M.; Kent, S. B. H.; Moos, W. H. *J. Am. Chem. Soc.* **1992**, *114*, 10646–10647.

(2) (a) Simon, R. J.; Kania, R. S.; Zuckermann, R. N.; Huebner, V. D.; Jewell, D. A.; Banville, S.; Ng, S.; Wang, L.; Rosenberg, S.; Marlowe, C. K. *Proc. Natl. Acad. Sci. U.S.A.* **1992**, *89*, 9367–9371. (b) Culf, A. S.; Ouellette, R. J. *Molecules* **2010**, *15*, 5282–5335.

(3) (a) Murnen, H. K.; Rosales, A. M.; Jaworski, J. N.; Segalman, R. A.; Zuckermann, R. N. *J. Am. Chem. Soc.* **2010**, *132*, 16112–16119. (b) Nam, K. T.; Shelby, S. A.; Choi, P. H.; Marciel, A. B.; Chen, R.; Tan, L.; Chu, T. K.; Mesch, R. A.; Lee, B.-C.; Connolly, M. D.; Kisielowski, C.; Zuckermann, R. N. *Nat. Mater.* **2010**, *9*, 454–460.

(4) Lee, B.-C.; Chu, T. K.; Dill, K. A.; Zuckermann, R. N. *J. Am. Chem. Soc.* **2008**, *130*, 8847–8855.

(5) (a) Lee, B.-C.; Zuckermann, R. N.; Dill, K. A. *J. Am. Chem. Soc.* **2005**, *127*, 10999–11009. (b) Burkoth, T. S.; Beausoleil, E.; Kaur, S.; Tang, D.; Cohen, F. E.; Zuckermann, R. N. *Chem. Biol.* **2002**, *9*, 647–654.

(6) Maayan, G.; Ward, M. D.; Kirshenbaum, K. *Proc. Natl. Acad. Sci. U.S.A.* **2009**, *106*, 13679–13684.

(7) (a) Murphy, J. E.; Uno, T.; Hamer, J. D.; Cohen, F. E.; Dwarki, V.; Zuckermann, R. N. *Proc. Natl. Acad. Sci. U.S.A.* **1998**, *95*, 1517–1522. (b) Huang, C.-Y.; Uno, T.; Murphy, J. E.; Lee, S.; Hamer, J. D.; Escobedo, J. A.; Cohen, F. E.; Radhakrishnan, R.; Dwarki, V.; Zuckermann, R. N. *Chem. Biol.* **1998**, *5*, 345–354. (c) Utku, Y.; Dehan, E.; Ouerfelli, O.; Piano, F.; Zuckermann, R. N.; Pagano, M.; Kirshenbaum, K. *Mol. BioSyst.* **2006**, *2*, 312–317. (d) Wender, P. A.; Mitchell, D. J.; Pattabiraman, K.; Pelkey, E. T.; Steinman, L.; Rothbard, J. B. *Proc. Natl. Acad. Sci. U.S.A.* **2000**, *97*, 13003–13008. (e) Schroder, T.; Niemeier, N.; Afonin, S.; Ulrich, A. S.; Krug, H. F.; Brase, S. *J. Med. Chem.* **2008**, *51*, 376–379.

(8) (a) Maayan, G.; Ward, M. D.; Kirshenbaum, K. *Chem. Commun.* **2009**, 56–58. (b) Cola, C. D.; Licen, S.; Comegna, D.; Cafaro, E.; Bifulco, G.; Izzo, I.; Tecilla, P.; De Riccardis, F. *Org. Biomol. Chem.* **2009**, *7*, 2851–2854.

(9) Maulucci, N.; Izzo, I.; Bifulco, G.; Aliberti, A.; Cola, C. D.; Comegna, D.; Gaeta, C.; Napolitano, A.; Pizza, C.; Tedesco, C.; Flot, D.; De Riccardis, F. *Chem. Commun.* **2008**, 3927–3929.

(10) (a) Chongsiriwatana, N. P.; Patch, J. A.; Czyzewski, A. M.; Dohm, M. T.; Ivankin, A.; Gidalevitz, D.; Zuckermann, R. N.; Barron,

A. E. *Proc. Natl. Acad. Sci. U.S.A.* **2008**, *105*, 2794–2799. (b) Comegna, D.; Benincasa, M.; Gennaro, R.; Izzo, I.; De Riccardis, F. *Biorg. Med. Chem.* **2010**, *18*, 2010–2018.

(11) (a) Reddy, M. M.; Wilson, R.; Wilson, J.; Connell, S.; Gocke, A.; Hynan, L.; German, D.; Kodadek, T. *Cell* **2011**, *144*, 132–142. (b) Zuckermann, R. N.; Kodadek, T. *Curr. Opin. Mol. Ther.* **2009**, *11*, 299–307.

(12) Kirshenbaum, K.; Barron, A. E.; Goldsmith, R. A.; Armand, P.; Bradley, E. K.; Truong, K. T. V.; Dill, K. A.; Cohen, F. E.; Zuckermann, R. N. *Proc. Natl. Acad. Sci. U.S.A.* **1998**, *95*, 4303–4308.

(13) (a) Armand, P.; Kirshenbaum, K.; Falicov, A.; Dunbrack, R. L.; Dill, K. A.; Zuckermann, R. N.; Cohen, F. E. *Folding Des.* **1997**, *2*, 369–375. (b) Pokorski, J. K.; Miller Jenkins, L. M.; Feng, H.; Durell, S. R.; Bai, Y.; Appella, D. H. *Org. Lett.* **2007**, *9*, 2381–2383. (c) Shin, S. B. Y.; Yoo, B.; Todaro, L. J.; Kirshenbaum, K. *J. Am. Chem. Soc.* **2007**, *129*, 3218–3225. (d) Fowler, S. A.; Luechapanichkul, R.; Blackwell, H. E. *J. Org. Chem.* **2009**, *74*, 1440–1449. (e) Gorske, B. C.; Blackwell, H. E. *J. Am. Chem. Soc.* **2006**, *128*, 14378–14387.

(14) (a) Huang, K.; Wu, C. W.; Sanborn, T. J.; Patch, J. A.; Kirshenbaum, K.; Zuckermann, R. N.; Barron, A. E.; Radhakrishnan, I. *J. Am. Chem. Soc.* **2006**, *128*, 1733–1738. (b) Gorske, B. C.; Stringer, J. R.; Bastian, B. L.; Fowler, S. A.; Blackwell, H. E. *J. Am. Chem. Soc.* **2009**, *131*, 16555–16567.

(15) Dill, K. A.; Bromberg, S.; Yue, K.; Chan, H. S.; Fiebig, K. M.; Yee, D. P.; Thomas, P. D. *Protein Sci.* **1995**, *4*, 561–602.

(16) (a) Yoo, B.; Kirshenbaum, K. *Curr. Opin. Chem. Biol.* **2008**, *12*, 714–721. (b) Fowler, S. A.; Blackwell, H. E. *Org. Biomol. Chem.* **2009**, *7*, 1508–1524. (c) Bautista, A. D.; Craig, C. J.; Harker, E. A.; Schepartz, A. *Curr. Opin. Chem. Biol.* **2007**, *11*, 685–692. (d) Gellman, S. H. *Acc. Chem. Res.* **1998**, *31*, 173–180. (e) Seebach, D.; Abele, S.; Gademann, K.; Jaun, B. *Angew. Chem., Int. Ed.* **1999**, *38*, 1595–1597. (f) Kendhale, A. M.; Poniman, L.; Dong, Z.; Laxmi-Reddy, K.; Kauffmann, B.; Ferrand, Y.; Huc, I. *J. Org. Chem.* **2010**, *76*, 195–200. (f) Hill, D. J.; Mio, M. J.; Prince, R. B.; Hughes, T. S.; Moore, J. S. *Chem. Rev.* **2001**, *101*, 3893–4012. (g) Horne, W. S.; Gellman, S. H. *Acc. Chem. Res.* **2008**, *41*, 1399–1408. (h) Margulies, D.; Hamilton, A. D. *Curr. Opin. Chem. Biol.* **2010**, *14*, 705–712. (i) Delsuc, N.; Massip, S.; Leger, J. M.; Kauffmann, B.; Huc, I. *J. Am. Chem. Soc.* **2011**, *133*, 3165–3172.

(17) In order to be consistent with peptide nomenclature we use the terms "*cis*" and "*trans*" to describe the amide dihedral angle omega (ω) referring to the relative positions of the backbone alpha carbons. For all *N*-aryl peptoids, "*trans*" amide conformation corresponds to the *E* isomer, while the "*cis*" amide corresponds to the *Z* isomer.

(18) Butterfoss, G. L.; Renfrew, P. D.; Kuhlman, B.; Kirshenbaum, K.; Bonneau, R. *J. Am. Chem. Soc.* **2009**, *131*, 16798–16807.

(19) Shah, N. H.; Butterfoss, G. L.; Nguyen, K.; Yoo, B.; Bonneau, R.; Rabenstein, D. L.; Kirshenbaum, K. *J. Am. Chem. Soc.* **2008**, *130*, 16622–16632.

(20) Stringer, J. R.; Crapster, J. A.; Guzei, I. A.; Blackwell, H. E. *J. Org. Chem.* **2010**, *75*, 6068–6078.

(21) Armand, P.; Kirshenbaum, K.; Goldsmith, R. A.; Farr-Jones, S.; Barron, A. E.; Truong, K. T. V.; Dill, K. A.; Mierke, D. F.; Cohen, F. E.; Zuckermann, R. N.; Bradley, E. K. *Proc. Natl. Acad. Sci. U.S.A.* **1998**, *95*, 4309–4314.

(22) Wu, C. W.; Kirshenbaum, K.; Sanborn, T. J.; Patch, J. A.; Huang, K.; Dill, K. A.; Zuckermann, R. N.; Barron, A. E. *J. Am. Chem. Soc.* **2003**, *125*, 13525–13530.

(23) Gorske, B. C.; Bastian, B. L.; Geske, G. D.; Blackwell, H. E. *J. Am. Chem. Soc.* **2007**, *129*, 8928–8929.

(24) (a) Choudhary, A.; Gandla, D.; Krow, G. R.; Raines, R. T. *J. Am. Chem. Soc.* **2009**, *131*, 7244–7246. (b) Bartlett, G. J.; Choudhary, A.; Raines, R. T.; Woolfson, D. N. *Nat. Chem. Biol.* **2010**, *6*, 615–620. (c) Choudhary, A.; Kamer, K. J.; Powner, M. W.; Sutherland, J. D.; Raines, R. T. *ACS Chem. Biol.* **2010**, *5*, 655–657. (d) Kuemin, M.; Nagel, Y. A.; Schweizer, S.; Monnard, F. W.; Ochsenfeld, C.; Wennemers, H. *Angew. Chem., Int. Ed.* **2010**, *49*, 6324–6327.

(25) Yoo, B.; Shin, S. B. Y.; Huang, M. L.; Kirshenbaum, K. *Chem. —Eur. J.* **2010**, *16*, 5528–5537.

(26) Dunbrack, R. L.; Karplus, M. *J. Mol. Biol.* **1993**, *230*, 543–574.

(27) Curran, D. P.; Qi, H.; Geib, S. J.; DeMello, N. C. *J. Am. Chem. Soc.* **1994**, *116*, 3131–3132.

(28) Clayden, J. *Chem. Commun.* **2004**, 127–135.

(29) (a) Clayden, J.; Lemiegre, L.; Morris, G. A.; Pickworth, M.; Snape, T. J.; Jones, L. H. *J. Am. Chem. Soc.* **2008**, *130*, 15193–15202. (b) Gaucher, A.; Dutot, L.; Barbeau, O.; Wakselman, M.; Mazaleyrat, J.-P.; Peggion, C.; Oancea, S.; Formaggio, F.; Crisma, M.; Toniolo, C. *Tetrahedron: Asymmetry* **2006**, *17*, 30–39. (c) Kim, I. C.; Hamilton, A. D. *Org. Lett.* **2006**, *8*, 1751–1754. (d) Mazaleyrat, J. P.; Wright, K.; Gaucher, A.; Toulemonde, N.; Wakselman, M.; Oancea, S.; Peggion, C.; Formaggio, F.; Setnicka, V.; Keiderling, T. A.; Toniolo, C. *J. Am. Chem. Soc.* **2004**, *126*, 12874–12879.

(30) Eliel, E. L.; Wilen, S. H. *Stereochemistry of Organic Compounds*; Wiley-Interscience: New York, 1994.

(31) Oki, M. *The Chemistry of Rotational Isomers*; Springer-Verlag: New York, 1993.

(32) Wolf, C. (Ed.) *Dynamic Stereochemistry of Chiral Compounds*, RSC Publishing: Cambridge, U.K., 2008.

(33) (a) Adams, R.; Yuan, H. C. *Chem. Rev.* **1933**, *12*, 261–338. (b) Clayden, J.; Westlund, N.; Frampton, C. S.; Helliwell, M. *Org. Biomol. Chem.* **2006**, *4*, 455–461. (c) Clayden, J. *Angew. Chem., Int. Ed.* **1997**, *36*, 949–951. (d) Guthrie, D. B.; Geib, S. J.; Curran, D. P. *J. Am. Chem. Soc.* **2010**, *133*, 115–122.

(34) Clayden, J.; Moran, W.; Edwards, P.; LaPlante, S. *Angew. Chem., Int. Ed.* **2009**, *48*, 6398–6401.

(35) Curran, D. P.; Hale, G. R.; Geib, S. J.; Balog, A.; Cass, Q. B.; Degani, A. L. G.; Hernandes, M. Z.; Freitas, L. C. G. *Tetrahedron: Asymmetry* **1997**, *8*, 3955–3975.

(36) Lapierre, A. J. B.; Geib, S. J.; Curran, D. P. *J. Am. Chem. Soc.* **2006**, *129*, 494–495.

(37) Gustafson, J. L.; Lim, D.; Miller, S. J. *Science* **2010**, *328*, 1251–1255.

(38) (a) Ates, A.; Curran, D. P. *J. Am. Chem. Soc.* **2001**, *123*, 5130–5131. (b) Adler, T.; Bonjoch, J.; Clayden, J.; Font-Bardia, M.; Pickworth, M.; Solans, X.; Sole, D.; Vallverdu, L. *Org. Biomol. Chem.* **2005**, *3*, 3173–3183. (c) Kitagawa, O.; Yoshikawa, M.; Tanabe, H.; Morita, T.; Takahashi, M.; Dobashi, Y.; Taguchi, T. *J. Am. Chem. Soc.* **2006**, *128*, 12923–12931. (d) Kitagawa, O.; Takahashi, M.; Yoshikawa, M.; Taguchi, T. *J. Am. Chem. Soc.* **2005**, *127*, 3676–3677.

(39) Kruijtzer, J. A. W.; Liskamp, R. M. J. *Tetrahedron Lett.* **1995**, *36*, 6969–6972.

(40) (a) Siddall, T. H. *J. Phys. Chem.* **1966**, *70*, 2249–2256. (b) Siddall, T. H. *J. Org. Chem.* **1966**, *31*, 3719–3725. (c) Siddall, T. H.; Stewart, W. E. *J. Org. Chem.* **1969**, *34*, 2927–2933. (d) Siddall, T. H.; Stewart, W. E. *J. Phys. Chem.* **1969**, *73*, 40–45. (e) Shvo, Y.; Taylor, E. C.; Mislow, K.; Raban, M. *J. Am. Chem. Soc.* **1967**, *89*, 4910–4917.

(41) Kim, Y.-J.; Park, Y.; Park, K. K. *J. Mol. Struct.* **2006**, *783*, 61–65.

(42) (a) Cass, Q. B.; Degani, A. L. G.; Tiritan, M. E.; Matlin, S. A.; Curran, D. P.; Balog, A. *Chirality* **1997**, *9*, 109–112. (b) Wolf, C. *Chem. Soc. Rev.* **2005**, *34*, 595–608.

(43) Ahmed, A.; Bragg, R. A.; Clayden, J.; Lai, L. W.; McCarthy, C.; Pink, J. H.; Westlund, N.; Yasin, S. A. *Tetrahedron* **1998**, *54*, 13277–13294.

(44) (a) Metrangolo, P.; Neukirch, H.; Pilati, T.; Resnati, G. *Acc. Chem. Res.* **2005**, *38*, 386–395. (b) Hardegger, L. A.; Kuhn, B.; Spinnler, B.; Anselm, L.; Ecabert, R.; Stihle, M.; Gsell, B.; Thoma, R.; Diez, J.; Benz, J.; Plancher, J.-M.; Hartmann, G.; Banner, D. W.; Haap, W.; Diederich, F. *Angew. Chem., Int. Ed.* **2011**, *50*, 314–318.

(45) (a) Clayden, J. *Chem. Soc. Rev.* **2009**, *38*, 817–829. (b) Dong, Z.; Plampin, J. N.; Yap, G. P. A.; Fox, J. M. *Org. Lett.* **2010**, *12*, 4002–4005.

(46) (a) Stone, M. T.; Fox, J. M.; Moore, J. S. *Org. Lett.* **2004**, *6*, 3317–3320. (b) Green, M. M.; Peterson, N. C.; Sato, T.; Teramoto, A.; Cook, R.; Lifson, S. *Science* **1995**, *268*, 1860–1866.

(47) Shin, S. B. Y.; Kirshenbaum, K. *Org. Lett.* **2007**, *9*, 5003–5006.

(48) Shah, N. H.; Kirshenbaum, K. *Org. Biomol. Chem.* **2008**, *6*, 2516–2521.

(49) Wang, J.; Feringa, B. L. *Science* **2011**, *331*, 1429–1432.